Lawrence Berkeley National Laboratory
Recent Work

Title

THE ASYMMETRIC GRAETZ PROBLEM IN CHANNEL FLOW

Permalink

https://escholarship.org/uc/item/7pq075sq

Authors

Edwards, V.
Newman, J.

Publication Date

1983-08-01

Lawrence Berkeley Laboratory

UNIVERSITY OF CALIFORNIA

Materials & Molecular Research Division

THE ASYMMETRIC GRAETZ PROBLEM IN CHANNEL FLOW

V. Edwards and J. Newman

August 1983

DISCLAIMER

The Asymmetric Graetz Problem

in Channel Flow

Victoria Edwards and John Newman

Materials and Molecular Research Division

Lawrence Berkeley Laboratory, and

Department of Chemical Engineering

University of California

Berkeley, California 94720

August 9, 1983

Abstract

A convenient representation of the solution to the asymmetric Graetz problem in channel flow is presented. The asymmetric Graetz problem in channel flow is similar to the classical Graetz problem of heat or mass transfer to a fluid flowing in a round duct. In the classical problem, the tube wall undergoes a step change in concentration at a given axial position. In the asymmetric Graetz problem, the duct is flat, and the concentration step occurs at only one channel wall. It is shown how this solution to the asymmetric Graetz problem may be used in a superposition integral to determine the wall flux in problems where the arbitrary channel wall concentrations differ on the two walls.

Introduction

The problem of mass transfer to fluids in laminar flow in ducts appears in many engineering applications. This problem has been solved for some special cases,[1-10] but here we shall consider the case of a flat duct, or channel, where the surface-concentration boundary conditions are arbitrary, and may differ on the two channel walls. This problem is of interest when the channel gap is thinner than the diffusion-boundary-layer thickness. In such cases, the fluxes at the two channel walls are not independent.

Since the detailed concentration profile within the flowing fluid is generally not needed, we shall emphasize the distribution of flux along the channel walls. Given this flux distribution, one can calculate the concentration at the exit by performing an overall material balance.

To obtain the distribution of flux along the two channel walls, it is necessary to solve the convective diffusion equation with arbitrary nonlinear concentration boundary conditions. Because the convective diffusion equation is linear, however, Duhamel's superposition principle may be used to treat the nonlinear boundary conditions. According to Duhamel's theorem, the solution to a linear problem with nonlinear boundary conditions may be written as a superposition of solutions to the problem with step-function boundary conditions.[11,12]

The symmetric problem, which has step-function boundary conditions on both walls, has been solved.[4-6] When the surface concentration profiles are different on the two walls, however, it is necessary to solve the asymmetric problem. In the asymmetric problem, there is a step function in concentration on only one wall. Yih and Cermak[7] and Schenk and Beckers[8] have treated this asymmetric problem, but their results are only applicable far from the step change in concentration. Hatton and Turton's results can be used over a somewhat larger range.[9]

Cess and Schaffer[10] solved the problem with a unit step change in flux, rather than concentration. The solution presented here is in the form of a function that is accurate at all axial positions. Therefore, when the surface concentrations are known at all axial positions, this function may be used in a superposition integral to determine the wall fluxes.

Problem Statement

The convective diffusion equation for a species i is

$$\mathbf{v} \cdot \nabla c_i = D_i \nabla^2 c_i .$$

(1)

For laminar flow in a channel, v_y is zero, and, if axial diffusion is negligible, $\partial^2 c_i / \partial x^2$ can be neglected (see figure 1). Therefore,

$$v_x \frac{\partial c_i}{\partial x} = D_i \frac{\partial^2 c_i}{\partial y^2} ,$$

(2)

where

$$v_x = \frac{3}{2} <v_x> \left[1 - \left(\frac{y}{B} \right)^2 \right]$$

(3)

and B is the channel halfwidth. The origin of the coordinate system is chosen to be in the center of the channel for convenience. .

Equation 2 may be written in dimensionless form by defining the variables

$$\theta = \frac{c_i - c_b}{c_o - c_b}$$

(4)

$$\xi = \frac{y}{B}$$

(5)

$$\zeta = x \frac{D_i}{\frac{3}{2} B^2 <v_x>} ,$$

(6)

where c_o is the surface concentration and c_b is the bulk concentration. Thus, the dimensionless convective diffusion equation is

$$(1 - \xi^2) \frac{\partial \theta}{\partial \zeta} = \frac{\partial^2 \theta}{\partial \xi^2} .$$

(7)

If the boundary conditions are arbitrary, Duhamel's superposition theorem may be used to write the flux in terms of the solution to the problem with a step-function concentration boundary con-

dition on one wall. For example, if wall "-1" is located at $\xi=-1$, and wall "1" is located at $\xi=1$, then the flux of species i at wall "-1" is

$$N_{i,-1}(x) = -\frac{D_i}{B}\int_0^x \frac{dc_{i,-1}}{dx}\Big|_{x^{\bullet}} \frac{\partial\theta}{\partial\xi}(\zeta-\zeta^{\bullet}, \xi=-1)\, dx^{\bullet} \tag{8}$$

$$+ \frac{D_i}{B}\int_0^x \frac{dc_{i,1}}{dx}\Big|_{x^{\bullet}} \frac{\partial\theta}{\partial\xi}(\zeta-\zeta^{\bullet}, \xi=1)\, dx^{\bullet},$$

where $c_{i,-1}$ is the surface concentration of species i at $\xi=-1$ and $c_{i,1}$ is the concentration of species i at $\xi=1$. The flux (in the $+\xi$ direction) of species i at wall "1" is obtained by reversing the wall subscripts and the signs:

$$N_{i,1}(x) = \frac{D_i}{B}\int_0^x \frac{dc_{i,1}}{dx}\Big|_{x^{\bullet}} \frac{\partial\theta}{\partial\xi}(\zeta-\zeta^{\bullet}, \xi=-1)\, dx^{\bullet} \tag{9}$$

$$- \frac{D_i}{B}\int_0^x \frac{dc_{i,-1}}{dx}\Big|_{x^{\bullet}} \frac{\partial\theta}{\partial\xi}(\zeta-\zeta^{\bullet}, \xi=1)\, dx^{\bullet}.$$

Both fluxes are in the positive ξ direction. In equations 8 and 9, $\theta(\zeta,\xi)$ is the solution to the dimensionless convective diffusion equation (equation 7) with boundary conditions

$$\theta = 1 \; at \; \xi = -1 \tag{10}$$

$$\theta = 0 \; at \; \xi = 1 \tag{11}$$

$$\theta = 0 \; at \; \zeta = 0 . \tag{12}$$

That is, θ has a unit step function boundary condition on wall "-1". The quantity $\partial\theta/\partial\xi$ at either wall is related to the Nusselt number (dimensionless flux) by

$$Nu = -2\, \frac{\partial\theta}{\partial\xi}, \tag{13}$$

where Nu is defined to be positive on both walls. Figure 2 illustrates the concentration profiles for this step-function boundary-condition problem.

The Lévêque Approach

In general, equation 2 must be solved numerically. If, however, the diffusion boundary layers are thin, an analytic solution for the flux can be obtained by assuming that the velocity profile is linear throughout the boundary layer. This approximation is known as the Lévêque approximation.[2,3,13,14] It should be noted that this approximation is not valid throughout a thin-gap channel, because the diffusion boundary layers can fill the entire gap and, hence, the velocity profiles are not linear. This approximation is useful, however, for treating the entrance region, where the diffusion boundary layers are thin. Norris and Streid have solved this Lévêque problem for channel flow.[6]

One can extend the range of applicability of the Lévêque solution by writing a Lévêque series for the Nusselt number. This has been done for the Graetz problem in a tube,[3,14] and a similar procedure may be used for a channel. (The procedure is illustrated for an annulus in problem 1 in chapter 17 of reference 13). The first three terms of the channel Lévêque series are:

$$Nu = -2 \frac{\partial \theta}{\partial \xi} \big|_{\xi=-1} = 1.35659745 \zeta^{-1/3} - 0.2 - 0.060733452 \zeta^{1/3} . \tag{14}$$

The Graetz Approach

To treat the downstream region, the Graetz approach (separation of variables) should be used. The boundary conditions (equations 10-12) can be simplified by subtracting the downstream linear concentration profile from the actual concentration profile. Thus we define

$$C = \theta - \theta_\infty = \theta - (\frac{1}{2} - \frac{\xi}{2}) . \tag{15}$$

The new variable C still satisfies the dimensionless convective diffusion equation, but the boundary conditions are symmetric and homogeneous:

$$C = 0 \text{ at } \xi = -1 \tag{16}$$

$$C = 0 \text{ at } \xi = 1 . \tag{17}$$

Using separation of variables transforms the partial differential equation into two ordinary differential equations:

$$\frac{dX}{d\zeta} = -\lambda^2 X \tag{18}$$

$$\frac{d^2Y}{d\xi^2} + \lambda^2 (1 - \xi^2) \, Y = 0 , \tag{19}$$

where

$$C = X(\zeta)Y(\xi) . \tag{20}$$

Equation 18 can be solved readily:

$$X = A \, e^{-\lambda^2\zeta} . \tag{21}$$

Equation 19, however, is an eigenvalue problem that must be solved numerically.

To calculate the complete solution for the dimensionless concentration,

$$\theta = \frac{1}{2} - \frac{\xi}{2} + \sum_{k=1}^{\infty} A_k \, e^{-\lambda_k^2\zeta} \, Y_k(\xi) , \tag{22}$$

the coefficients A_k, the eigenvalues λ_k, and the eigenfunctions Y_k are needed. The coefficients are obtained by using the orthogonality of the eigenfunctions with respect to the weight function $(1-\xi^2)$. Since $\theta = 0$ at $\zeta = 0$,

$$A_k = \frac{-\int_{-1}^{1} (1-\xi^2) \, Y_k(\xi) \, (\frac{1}{2} - \frac{\xi}{2}) \, d\xi}{\int_{-1}^{1} [Y_k(\xi)]^2 \, (1 - \xi^2) \, d\xi} . \tag{23}$$

Equation 23 may be simplified because the eigenfunctions are either odd or even functions in ξ. Thus, if $Y_k(\xi)$ is an odd function,

$$A_k = \frac{\int\limits_0^1 \xi\,(1-\xi^2)\,Y_k(\xi)\,d\xi}{2\int\limits_0^1 Y_k^2(\xi)\,(1-\xi^2)\,d\xi}\,. \tag{24}$$

If $Y_k(\xi)$ is an even function,

$$A_k = \frac{-\int\limits_0^1 (1-\xi^2)\,Y_k(\xi)\,d\xi}{2\int\limits_0^1 Y_k^2(\xi)\,(1-\xi^2)\,d\xi}\,. \tag{25}$$

The eigenvalues and eigenfunctions must be obtained numerically from the eigenvalue problem

$$\frac{d^2Y}{d\xi^2} + \lambda^2\,(1-\xi^2)\,Y = 0\,, \tag{26}$$

with boundary conditions

$$Y = 0 \text{ at } \xi = -1 \tag{27}$$

$$Y = 0 \text{ at } \xi = 1\,. \tag{28}$$

Solution of the Eigenvalue Problem

One can rewrite the eigenvalue problem in a form convenient for numerical solution by realizing that the eigenvalues λ are constant. Thus,

$$Y'' + \lambda^2(1-\xi^2)Y = 0 \tag{29}$$

$$\frac{d\lambda^2}{d\xi} = 0\,, \tag{30}$$

where the primes denote differentiation with respect to ξ. To solve equations 29 and 30, three boundary conditions are needed. The first two boundary conditions are stated in equations 27 and 28. The third boundary condition is a normalization condition

$$Y' = 1 \text{ at } \xi = 1 . \tag{31}$$

This boundary condition can be imposed because the eigenfunctions are multiplied by the constants A_k. Thus, the eigenfunctions may be chosen such that Y_k' has the same value for all k. Naturally, Y_k' cannot be chosen to be infinite or zero because the wall flux is finite. Note that equations 29 and 30, with boundary conditions 27, 28, and 31, are satisfied only for certain discrete eigenvalues λ_k.

The system of two ordinary differential equations with the three boundary conditions can be solved numerically using a finite-difference technique.[14,15]

The results of this procedure are tabulated in Tables I and II. A plot of the Graetz functions for the asymmetric channel problem is shown in figure 3; the corresponding eigenvalues are shown in figure 4. Note that half of the eigenfunctions are even in ξ, and half of them are odd.

Comparison with Literature

Tables I and II show the eigenvalues and coefficients as calculated by various authors. The second column shows the accurate results of Brown for the even eigenfunctions.[4] The third column contains the asymmetric-boundary-condition results of Hatton and Turton,[9] and the fourth column contains the results of Yih and Cermak.[7] To calculate the coefficients, A_k, from Yih and Cermak's work, it was necessary to estimate $Y_k'(1)$ from the tables and graphs of Y_k. Sellars, Tribus, and Klein have presented a method for calculating the higher eigenvalues.[5] The fifth column in tables I and II and figure 4 show the results of their procedure.

Combining the Graetz and Lévêque Solutions

It should be noted that a truncated Graetz series (obtained from equation 22) is accurate for large ζ, while the Lévêque series (equation 14) is valid for small ζ. The value of ζ that divides the two regions is that value at which the ratio of the two asymptotic solutions is closest to unity. If more terms are used in the Graetz series, this value of ζ becomes smaller, and the

accuracy is improved. Similarly, the accuracy can be improved by adding more terms to the Lévêque series; then the value of ζ dividing the two regions becomes larger. By adding more terms to each of the two series, any desired degree of accuracy can be obtained. If three terms are used in each series, the maximum error in the Nusselt number is 0.48%. This maximum error occurs at $\zeta = 0.11$, the value that divides the two regions.

Asymptotic Forms for Large Eigenvalues

If greater accuracy than 0.48% is desired, then it is most efficient to add terms to the Graetz series. Therefore, it is useful to have simple asymptotic forms for calculating the higher eigenvalues and corresponding coefficients.

For the Graetz problem in a tube, Newman[14] extended the asymptotic forms of Sellars *et al.*[5] to achieve accuracy over a greater range of eigenvalues. Using a similar procedure, we devised an asymptotic form for the asymmetric Graetz problem:

$$\lambda = \lambda_0 + \frac{0.03254}{\lambda_0^{4/3}} - \frac{0.11}{\lambda_0^{14/3}} , \tag{32}$$

where

$$\lambda_0 = \frac{6k - 1}{3} \qquad \text{for } k = 1, 2, \cdots \tag{33}$$

is the asymptotic form obtained by modifying the method of Sellars *et al.* (see reference 9). The function in equation 32 may be used for $\lambda_6, \lambda_7, \ldots$, with a maximum error of $10^{-5}\%$.

The method of Sellars *et al.* predicts that the coefficients behave as $A_k = (-1)^{k+1} K / \lambda_k^{1/3}$ as λ_k becomes large, where

$$K = \frac{2^{4/3} \, \Gamma(\frac{2}{3})}{3^{1/6} \, \Gamma(\frac{4}{3}) \, \pi} = 1.012787288 . \tag{34}$$

This asymptotic form was modified to

$$A_k = (-1)^{k+1} \left(\frac{K}{\lambda_k^{1/3}} \right)(1 + 0.03\lambda_k^{-4/3} - 0.03\lambda_k^{-8/3}) \ . \tag{35}$$

Equation 35 gives a maximum error of $4 \times 10^{-4}\%$ for $k \geq 6$.

Table III shows the comparison between the eigenvalues as calculated by solving the eigen-value problem and the eigenvalues as calculated from the asymptotic form in equation 32. Table IV shows the comparison for the coefficients.

By using these asymptotic forms in a Graetz series with many terms, one can achieve a high degree of accuracy in the Nusselt number. For example, if the most accurate eigenvalues and coefficients from tables I and II are used for $k \leq 5$, Brown's coefficients are used for $k = 7,9,11$, and the asymptotic forms are used everywhere else, a 100-term Graetz series can be used down to $\zeta = 2.9 \times 10^{-4}$, with a maximum error in Nu of $7.5 \times 10^{-4}\%$. If a 3-term Graetz series is used, the maximum error between the Graetz and Lévêque series is 0.48%.

Empirical Approach

Recall that the Lévêque solution is only applicable on the wall with the step change in con-centration. To fit the region of small ζ on the opposite wall, it is more convenient to use an empirical function than it is to use a very large number of terms in the Graetz series.

The empirical function used here was derived by considering a simpler problem. If the fluid were in plug flow, rather than laminar flow, the mass-transfer problem would be analogous to the problem of transient heat conduction in a finite slab. If the temperature at one wall undergoes a step change at time $t = 0$, the flux at the opposite wall increases with time. In the channel-flow problem, the flux increases with distance down the channel. Thus, the short-time solution is analogous to the small-ζ solution.

Based on the short-time solution for heat conduction in a finite slab, it is assumed that Nu is proportional to $e^{-b/\zeta}$. This assumption can be tested by plotting the Graetz-series form of Nu (using a large number of terms). Indeed the plot of $\ln Nu$ vs. $1/\zeta$ is linear at high $1/\zeta$, and

this linear asymptote has a nonzero intercept. Therefore, at high $1/\zeta$, $\ln Nu$ is approximately $a-b/\zeta$, where a is approximately 1.0 and b is approximately 0.6. To match the behavior at low $1/\zeta$, a correction term of the form $ce^{-d/\zeta}$ can be added, where the constants c and d are estimated from a plot of $\ln(a - b/\zeta - \ln Nu)$ vs. $1/\zeta$. A better estimate of the constants was obtained by performing a least squares fit between $\ln Nu$ as calculated from a 100-term Graetz series and $\ln Nu = a - b/\zeta - ce^{-d/\zeta}$, for various specified values of d. The least squares fit was designed to weight the region of small ζ, where the empirical function is to be used. The value of d was chosen to make the maximum absolute error as small as possible, while keeping the maximum relative error at a very small value of ζ, where Nu is small. The resulting fitting function for small ζ is

$$Nu = -2 \frac{\partial \theta}{\partial \xi}\Big|_{\xi=1} = exp\left(0.9594 - 0.6069 \frac{1}{\zeta} - 0.4512 e^{-0.276/\zeta}\right). \tag{36}$$

In the region of small ζ ($\zeta < 0.3$), the maximum absolute error between this function and the 100-term Graetz-series representation of the Nusselt number is 2.3×10^{-4}. This maximum absolute error occurs at $\zeta = 0.25$. Here, the relative error is 0.11%. The maximum relative error is 0.2%, and it occurs at $\zeta = 0.05$.

Recall that equation 36 is applicable only at small ζ, and the truncated Graetz series is applicable only at large ζ. Again, we choose to use a 3-term Graetz series. Comparison of this series with the 100-term series shows that the 3-term series is comparable in accuracy to the empirical function for $\zeta \geq 0.16$. Actually, however, the empirical function is superior to the 3-term Graetz series for $0.16 < \zeta < 0.18$. Therefore, the value of ζ dividing the two regions was chosen to be 0.18. Here, the error between the 3-term Graetz series and the empirical function is 0.013%.

Summary of Results

In summary, a convenient representation of the Nusselt number for the asymmetric Graetz problem has been obtained. For the wall with the step change in concentration:

$$Nu = 1.35659745\zeta^{-1/3} - 0.2 - 0.060733452\zeta^{1/3} \qquad \text{for } \zeta < 0.11 \qquad (37)$$

$$Nu = 1 + 2\sum_{k=1}^{3} |A_k| \, e^{-\lambda_k^2 \zeta} \qquad \text{for } \zeta \geq 0.11, \qquad (38)$$

where

$$A_1 = 0.8580866740 \qquad\qquad \lambda_1 = 1.6815953222 \qquad (39)$$

$$A_2 = -0.65921993 \qquad\qquad \lambda_2 = 3.6722904 \qquad (40)$$

$$A_3 = 0.5694628499 \qquad\qquad \lambda_3 = 5.6698573459 . \qquad (41)$$

For the wall without the step change:

$$Nu = exp\left(0.9594 - 0.6069 \frac{1}{\zeta} - 0.4512 e^{-0.276/\zeta}\right) \qquad \text{for } \zeta < 0.18 \qquad (42)$$

$$Nu = 1 - 2\sum_{k=1}^{3} A_k e^{-\lambda_k^2 \zeta} \qquad \text{for } \zeta \geq 0.18. \qquad (43)$$

It has been shown that this solution may be used in a superposition integral to determine the wall flux in problems where the channel wall concentrations are arbitrary and may differ on the two walls.

Acknowledgment

List of Symbols

A	coefficient in eigenfunction expansion of concentration
B	channel halfwidth, cm
c_b	bulk concentration of species i, mol/cm^3
c_i	concentration of species i, mol/cm^3
c_o	surface concentration of species i, mol/cm^3
C	dimensionless concentration defined in equation 20
D_i	diffusion coefficient of species i, cm^2/s
K	constant defined in equation 34
Nu	Nusselt number $= \dfrac{\partial c_i}{\partial y} \dfrac{2B}{c_b - c_o}$
v	fluid velocity, cm/s
v_x	component of velocity in the axial direction, cm/s
v_y	component of velocity in the normal direction, cm/s
x	axial coordinate, cm
X	axial dependence of concentration, defined in equation 20
y	normal coordinate, cm
Y	normal dependence of concentration, defined in equation 20

Greek

ζ	dimensionless axial coordinate defined in equation 6
θ	dimensionless concentration defined in equation 4
θ_∞	downstream dimensionless concentration (see equation 15)
λ	eigenvalue in equation 19
ξ	dimensionless normal coordinate defined in equation 5

Subscripts

b	refers to bulk solution
i	refers to a particular species in solution
k	summation index in eigenfunction expansion (see equation 22)
o	refers to wall surface
∞	downstream
-1	wall located at $\xi = -1$
1	wall located at $\xi = 1$
0	refers to asymptotic solution of Sellars *et al.*[5]

Superscripts

*	dummy variable of integration

List of Figures

List of Tables

References

1. L. Graetz, "Über die Wärmeleitungsfähigkeit von Flüssigkeiten," *Annalen der Physik und Chemie,* **18,** 79-94 (1883), **25,** 337-357 (1885).

2. M. A. Lévêque, "Les Lois de la Transmission de Chaleur par Convection," *Annales des Mines, Memoires,* ser. 12, **13,** 201-299, 305-362, 381-415 (1928).

3. John Newman, "Extension of the Lévêque Solution," *Transactions of the ASME, Part C, Journal of Heat Transfer,* **91,** 177-178 (February, 1969).

4. George Martin Brown, "Heat or Mass Transfer in a Fluid in Laminar Flow in a Circular or Flat Conduit," *A.I.Ch.E. Journal,* **6,** 179-183 (June, 1960).

5. J. R. Sellars, Myron Tribus, and J. S. Klein, "Heat Transfer to Laminar Flow in a Round Tube or Flat Conduit - The Graetz Problem Extended," *Transactions of the ASME,* 441-448 (February, 1956).

6. R. H. Norris and D. D. Streid, "Laminar-Flow Heat-Transfer Coefficients for Ducts," *Transactions of the ASME,* 525-533 (August, 1940).

7. C. S. Yih and Jack E. Cermak, "Laminar Heat Convection in Pipes and Ducts," Civil Engineering Department, Colorado Agricultural and Mechanical College, Fort Collins, Colorado (September, 1951). ONR Contract Number N90nr-82401, NR063-071/1-19-49.

8. J. Schenk and H. L. Beckers, "Heat Transfer in Laminar Flow between Parallel Plates," *Applied Scientific Research,* A4, 405-413 (1954).

9. A. P. Hatton and J. S. Turton, "Heat Transfer in the Thermal Entry Length with Laminar Flow between Parallel Walls at Unequal Temperatures," *International Journal*

of Heat and Mass Transfer, **5**, 673-679 (1962).

10. R. D. Cess and E. C. Shaffer, "Laminar Heat Transfer betweeen Parallel Plates with an Unsymmetrically Prescribed Heat Flux at the Walls," *Applied Scientific Research*, A9, 64-70 (1959).

11. Francis B. Hildebrand, *Advanced Calculus for Applications, Second Edition*, pp. 463-466, Prentice-Hall, Englewood Cliffs, New Jersey (1976).

12. C. Ray Wylie, *Advanced Engineering Mathematics, Fourth Edition*, pp. 309-319, McGraw Hill, New York (1960).

13. John Newman, *Electrochemical Systems*, pp. 311-316, Prentice-Hall, Englewood Cliffs, New Jersey (1973).

14. John Newman, "The Fundamental Principles of Current Distribution and Mass Transport in Electrochemical Cells," *Electroanalytical Chemistry, Volume 6*, Allen J. Bard, ed., pp. 196-221, Marcel Dekker, New York (1973).

15. John Newman, "Numerical Solution of Coupled, Ordinary Differential Equations," *Industrial and Engineering Chemistry Fundamentals*, **7**, 514-517 (August 1968).

Table I

Eigenvalues, λ_k

k	Present Work	Brown	Hatton and Turton	Yih and Cermak	Sellars, Tribus, and Klein
1	1.6815953	1.6815953222	1.681595	1.681	1 2/3
2	3.6722904		3.672290	3.673	3 2/3
3	5.6698573	5.6698573459	5.669858	5.670	5 2/3
4	7.6688088		7.668809	7.669	7 2/3
5	9.6682424	9.6682424625	9.668243	9.669	9 2/3
6	11.667894		11.66790	11.60	11 2/3
7	13.667661	13.6676614426	13.66766		13 2/3
8	15.667496		15.66750		15 2/3
9	17.667374	17.6673735653	17.66738		17 2/3
10	19.667279		19.66729		19 2/3

Table II

Coefficients, A_k

k	Present Work	Brown	Hatton and Turton	Yih and Cermak	Sellars, Tribus, and Klein
1	0.85808668	0.8580866740	0.8580871	0.8582	0.85421788
2	-0.65921993		-0.6592200	-0.6490	-0.65679187
3	0.56946285	0.5694628499	0.5694628	0.5665	0.56807937
4	-0.51452221		-0.5145219	-0.5060	-0.51362882
5	0.47606547	0.4760654555	0.4760652	0.4429	0.47543665
6	-0.44701873		-0.4470184	(-0.1142)	-0.44654920
7	0.42397373	0.4239737298	0.4239739		0.42360789
8	-0.40504973		-0.4050497		-0.40475545
9	0.38910871	0.3891087061	0.3891088		0.38886606
10	-0.37541429		-0.3754147		-0.37521022

Table III

Eigenvalues, λ_k

k	Calculated	Asymptotic
1	1.6815953	1.6729924
2	3.6722904	3.6721659
3	5.6698573	5.6698540
4	7.6688088	7.6688110
5	9.6682424	9.6682441
6	11.667894	11.667895
7	13.667661	13.667662
8	15.667496	15.667496
9	17.667374	17.667374
10	19.667279	19.667280

Table IV

Coefficients, A_k

k	Calculated	Asymptotic
1	0.85808668	0.85807016
2	-0.65921993	-0.65931889
3	0.56946285	0.56949143
4	-0.51452221	-0.51453243
5	0.47606547	0.47606966
6	-0.44701873	-0.44702059
7	0.42397373	0.42397459
8	-0.40504973	-0.40505013
9	0.38910871	0.38910889
10	-0.37541429	-0.37541436
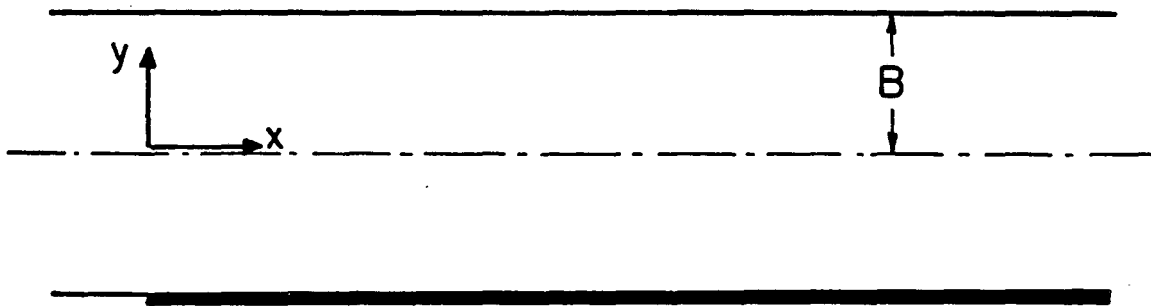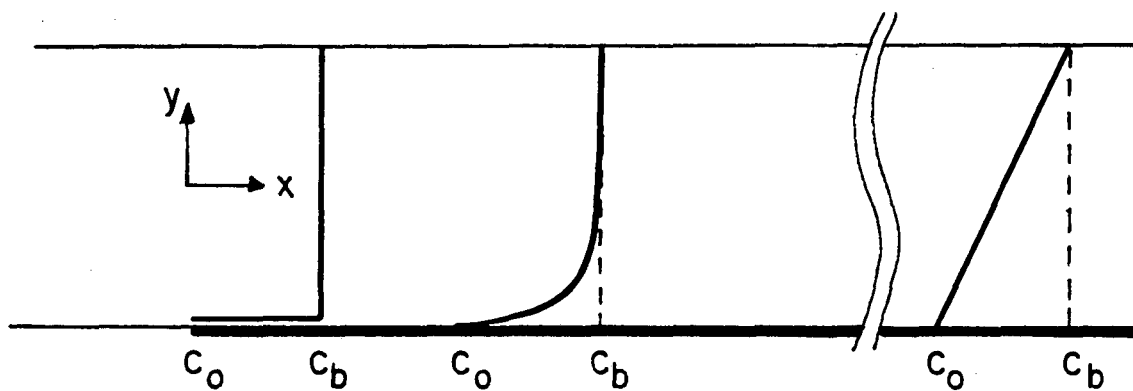
Figure 1.,

XBL 836-5845

Figure 2.

XBL 836-5846

Figure 3.

XBL 836-5847

Figure 4.